Characterization of the ocelli of the migratory Bogong moth (*Agrotis infusa*) in comparison to the non-migratory Turnip moth (*Agrotis segetum*)

Denis Vaduva

Abstract

The Bogong and Turnip moths are two species of the genus *Agrotis*, similar in size, but different in life style. The Bogong moth is a long distance migratory species endemic to Australia, whereas the Turnip moth has a wide spread in Africa, Europe and Asia where it is considered a pest. The ocelli are single-lens eyes of the camera type, whose role is still unknown in many insects, including the studied species. The present study searched for a potential role of these visual organs in these species, by determining the physiological and optical characteristics of the ocelli. Because of their different life styles (migratory vs. non-migratory), we searched to see if any differences are found and if the roles of the ocelli may differ as well. In my thesis I have found that these species have two underfocused ocelli placed laterally on the vertex of the head, close to the dorsal margin of the compound eyes and posterior to the antennae. The lenses are smooth with no pronounced asymmetry and astigmatism. The projection fields from the Bogong ocellar neurons are located close to the posterior brain surface, adjacent to the esophageal hole, anterior to the mushroom body calyx and anterior of the central complex. Because of the optical and physiological characteristics of the ocelli, it is probable that they play a role in flight stabilization reflexes although a function as a regulator of the initiation and cessation of diurnal activities, cannot be excluded.

Introduction

The Bogong (*Agrotis infusa*) and Turnip (*Agrotis segetum*) moths have a similar size and appearance and belong to the genus *Agrotis*. With a body length between 20 and 25 mm and wing span that is approximately 40-50 mm (Britton; CSIRO; Warrant et al., 2016), the Bogong moth is found in Australia and occasionally in Tasmania and New Zealand (Warrant et al., 2016). A nocturnal navigator, *Agrotis infusa* makes a spring migration of up to 1000 km from their breeding sites in southern Queensland, western and northwestern New South Wales (NSW) and western Victoria to their cool estivation caves in the alpine regions of NSW and Victoria where they “hibernate” over the summer months. In early autumn, a reverse migration occurs (Britton; Warrant et al., 2016).

Agrotis segetum is slightly smaller with a body length of 18-22 mm and wing span of 34-45 mm. Although a common European species, the Turnip moth has a wide distribution in Europe, Asia and Africa (The Cooperative Research Centre for National Plant Biosecurity) where it is considered a polyphagous pest (Chumakov and Kuznetsova, 2008).

General morphology of the ocelli in insects

As many insects, the Bogong and Turnip moths have a two-pathway visual system: the compound eyes and the ocelli (Berry et al., 2011). The ocelli are single-lens eyes of the camera type found in nymphal and adult hemimetabolous insects and adult holometabolous insects (Dickens and Eaton, 1974; Dickens and Eaton, 1973;

Warrant et al., 2006). The ocellus has a simple structure composed of a pigmented cone-shaped extension of the cuticle, a dome-like corneal lens and a retina separated from the lens by a layer of corneagen cells (Caldwell et al., 2007; Dickens and Eaton, 1974; Dow and Eaton, 1976; Horie et al., 2008; Toh and Okamura, 2007).

Typical for visual sensors in general, the number of ocelli varies between species (Vrsansky, 2008). Most commonly, such as in bees (Berry et al., 2011), wasps (Warrant et al., 2006), dragonflies (Berry et al., 2007a) and flies (Caldwell et al., 2007; Chen and Hua, 2014), the ocelli occur as a triplet and are generally located on the apex of the head between the compound eyes (Berry et al., 2007) whereas in locusts (Wilson, 1978) the median ocellus of the locust is directed forwards (Stange, 1981). Other species have only one ocellus, whereas species such as beetles lack them completely (Kalmus, 1946), and in some moth species within the families Sphingidae and Saturniidae, internal ocelli have been discovered (Dickens and Eaton, 1974; Dickens and Eaton, 1973; Dow and Eaton, 1976; Eaton, 1971) which may monitor light spread inside the head capsule (Eaton, 1971; Pappas and Eaton, 1977). Several moth species, have two ocelli positioned laterally on the vertex of the head, close to the dorsal margin of the compound eyes and posterior to the antennae (Grunewald and Wunderer, 1996; Pappas and Eaton, 1977).

Proposed functions of the ocelli

Despite the intense research and their apparent simplicity, a singular explanation for the function of the ocelli has remained elusive (Berry et al., 2007b; Warrant et al., 2006; Wilson, 1978). Generally, the ocelli have broad visual fields that partially overlap (Wilson, 1978; Taylor et al., 2016) and the images produced are underfocused, as the image plane appears to lie well behind the retinal layer (Mizunami, 1994). All this led to the creation of the "single sensor model" (Stange et al., 2002) in which, each ocellus is a highly sensitive optical sensor optimized for detecting illumination levels, providing rapid response through the ocellar large second order neurons (L-neurons). Thus, together, the ocelli act as an autopilot system with which the pitch, yaw and roll flight components are stabilized (Berry et al., 2011). This is furthermore improved by the fact that many ocelli have two spectral sensitivity peaks in the green and UV regions (Eaton, 1976; van Kleef et al., 2005; Yamazaki and Yamashita, 1991) and within the UV sensitivity range, the world is visible as only a bright sky and a dark ground (Wilson, 1978).

The function of the ocelli in flies

The structure and the neural organization of the ocellar system varies so much among insects (Mizunami, 1994; Mizunami, 1995) that a role as a single sensor is likely not the only role the ocelli may fulfill. In insects such as the fly *Drosophila*, the ocelli contribute to positive phototactive orientation mediated by the compound eyes, by adjusting their sensitivity (Hu and Stark, 1980; Mizunami, 1994). The ocelli also have a guiding role in houseflies, which are able to walk toward edges and relatively small bright objects placed in the frontal equatorial part of the visual field with their eyes completely occluded (Wehrhahn, 1984).

The role of the ocelli as polarized light detectors

Many insect species such as honeybees, desert ants, monarch butterflies, dung beetles and many others are able to orient by using specialized ommatidia in the dorsal rim areas of the compound eyes to detect the celestial patterns of light polarization (Wehner and Strasser, 1985; el Jundi et al., 2014). The western bumblebees, *Bombus occidentalis*, are able to use their ocelli alone or in conjunction

with the tops of its compound eyes to detect celestial polarized light and use it to prolong its foraging period at twilight (Wellingt. WG, 1974).

The desert ant, *Cataglyphis bicolor*, is also able to do this. By using only their ocelli and the patterns of polarized light, individuals of this species are able to find their way back home (Fent and Wehner, 1985). Similarly, the ocelli of the Australian desert ant *Melophorus bagoti*, provide celestial compass information for directional orientation, although, by themselves they are unable to mediate path integration. It is still unknown whether the directional information comes from polarized skylight, the sun's position or the color gradient of the sky (Schwarz et al., 2011a;Schwarz et al., 2011b).

The controlling role in diurnal activities of the ocelli in moths

In insects, light intensity levels often control the initiation and cessation of diurnal actives. This makes it advantageous to be able to detect minute changes in illumination. Thus, the high sensitivity of the ocelli, higher than that of the compound eyes, makes them perfectly suited as circadian controllers of diurnal activities (Mizunami, 1994). In bees, occlusion of the ocelli interferes with the timing of the first and last foraging flights, as the light intensity required increases with the number of non-functional ocelli (Lindauer and Schricker, 1963; Schricker, 1965).

The ocelli of the field crickets *Teleogryllus commodus*, and house crickets, *Acheta domesticus*, have a modulatory function, augmenting the sensitivity of the compound eyes to better perceive photic entrainment signals (Rence et al., 1988)

The ocelli perform an important function in the regulation of diurnal activities in the Cabbage looper moths, *Trichoplusia ni*, as well. Ocellar occlusion delays the flight initiation on the first day following emergence, but becomes less effective with time. However, ocellar ablation produces a permanent flight initiation delay (Eaton et al., 1983). The ocelli also regulate the intensity of the flight activity as anocellate males flew significantly less than control and sham-operated males. These males also had difficulties in adjusting to changes in the time of sunset as they performed worse than the males with intact ocelli (Sprint and Eaton, 1987). The ocelli of the Arctiid moth, *Creatonotos transiens*, also play a role in diurnal activities. Thus, when the control of the mating system of this species was studied, the occlusion of the ocelli, produced a significant delay in the onset of the luring activity. However, as this activity is only retarded, the compound eyes may be involved too (Wunderer and Dekramer, 1989).

The aim of the present study

Despite the recent research, the role of the ocelli still remains unknown in many species. The purpose of the present study is to determine the physiological and optical characteristics of the ocelli in the Bogong moth *Agrotis infusa*, and the Turnip moth *Agrotis segetum*. These were studied in order to find a potential role of these visual organs in these species and if any differences between them exist. These two species were chosen because of their close evolutionary relationship and different lifestyles. It is still unknown what role is played by the ocelli during the migration of the bogong moths, if any. The Turnip moth, with its nonmigratory lifestyle, serves as a comparison species, where, most probably, any differences are caused by differences in their lifestyles (migratory vs. nonmigratory).

Material and methods

Studied specimens

Turnip moth individuals were obtained from a laboratory culture maintained at the Department of Ecology in Lund, Sweden.

The culture was established 37 years ago from field-collected moths from southern Sweden and Denmark. The individuals were kept in a L17:D7 photoperiod at 22°C and 60% RH (relative humidity).

Bogong moth individuals were collected by Eric Warrant, Stanley Heinze, Kristina Brauburger, and Anna Stoeckl from an alpine cave in Mt. Kosciusko National Park, close to South Ramshead in early January 2013 and 2014. These individuals were kept in an incubator at Lund University in simulated cave conditions: lights on: 8pm to 12am (L16:D8), with 6 degrees at night and 10 degrees during the day and RH ca 75%.

Characterization of external morphology

Stereomicroscopy

The external morphology of the ocelli was studied using a Nikon SMZ18 stereomicroscope, by taking multiple Z-stacks which were then processed in NIS-Elements software, in order to obtain images with a large depth of field. The resulting images have all the different regions of the ocelli in focus.

Bogong and Turnip moth individuals were mounted on a holder using electrical tape and wax. In order to provide better access to the ocelli, the majority of the scales on the head were manually removed. Both males and females were used for this procedure.

In order to anesthetize the individuals prior to mounting, a male and a female Bogong moth were placed in the freezer for 20-30 minutes. These individuals were then kept further in the refrigerator for three days, over the weekend. After this period additional imaging sessions occurred. Two additional males were anesthetized using carbon dioxide from a Soda Stream machine, prior to mounting and photographing.

Scanning electron microscopy (SEM)

The external morphology of the Bogong ocelli was further studied with the help of scanning electron microscopy. Two series of SEM scanning occurred. First, four already dead individuals (two males and two females) were taken from the Bogong moth cage. Out of these, the scales on the head of one male and one female were manually removed in order to make the ocelli more visible. For the second session, two freshly killed males and one already dead female were used. The female was used previously in the stereomicroscopy study and was kept in the refrigerator at 4^0C. All three individuals had the scales completely removed.

All the individuals were fixed in a solution composed of 2% paraformaldehyde and 2.5% glutalaldehyde in 0.1 M sodium Cacodylate buffer. The samples were then dehydrated in a graded ethanol series and critical point dried, prior to being sputter-coated with gold.

Characterization of internal morphology

Paraffin embedding and sectioning

Prior to paraffin embedding, cryo-sectioning and plastic embedding, microscope slides were coated in a kromalungelatine solution (1g gelatin, 0,1g kromalun CrK(SO4)2*12H^{2}O, 200ml distilled H_2O) and dried overnight in the oven at 60^0C.

A total of seven Bogong moth heads with the antennae, mouth pieces and scales removed, were fixated overnight in two solutions: three males and one female in AFA II (alcohol-formaldehyde-acetic acid: 75 ml ethanol of 96% concentration, 20 ml of concentrated formaldehyde 37%, 5 ml of glacial acetic acid) and two females and one male in 10% neutral buffered formaldehyde (37% formaldehyde diluted

ten times in phosphate-buffered saline – PBS).

The fixated samples were rinsed in distilled water (3 x 10 minutes) followed by a dehydration in an ascending ethanol series (70% 2x15 min, 90% 2x15 min – AFI samples only, 96% 2x10 min and 100% 2x10 min). The dehydrated samples were incubated in xylene (2 x 10 min) and xylene/ paraffin (1:1 30 min) in the oven, followed by 3 changes of infiltration with fresh paraffin in (I x 1 h, II x overnight, III x 1h) in the oven at 60^0C. These samples were in turn embedded in a paraffin block inside a handmade paper form with a pre-established orientation (both horizontal and vertical planes of the ocelli were sliced). The samples were left in room temperature to harden.

The excess paraffin was removed from the blocks containing the samples so that two parallel sides were obtained. These, were sectioned using a rotation microtome in slices with a thickness of 5 μm. The result is a stripe of paraffin sections, which stick to each other. These in turn need to be "stretched out" as the samples are slightly compressed, by placing the sections in water drops on a kromalungelatine coated microscope slide placed on a warm plate. This water must be warm enough so that the paraffin stripes stretch out, but not too warm so that the paraffin will melt. After this is achieved, the excess water is removed and the samples are left to dry overnight. The sectioned samples were then deparaffinized by going through a series of xylene (2 x 5 min) and a descending ethanol series (100% 2 x 3 min, 95% 2 x 3 min, 70% 1 x 3 min, 50% 1 x 3 min) finishing with a rinsing in distilled water (1 x 3-5 min).

The deparaffinized samples were stained for at least 1 minute in a toluidine blue solution (Toluidine 0.5g, Sodium Borate – Borax 1.91g, distilled water 200 ml). Following the staining process, the samples were rinsed in an ascending ethanol series (70% ethanol – quick rinse to differentiate the tissue, 96% ethanol 1-2 min, 100% ethanol 2x5 min) and xylene (2x5 min) finishing with the mounting of a coverslip with New Entellan.

Cryo sectioning

A total of three Bogong moth heads with the antennae, mouth pieces and scales removed, were fixated overnight in two solutions: two males in AFA II (75% ethanol of 96% concentration, 20% of concentrated formaldehyde 37%, 5% of glacial acetic acid) and 1 female in 10% neutral buffered formaldehyde (37% formaldehyde diluted ten times in phosphate-buffered saline – PBS).

After the fixation was completed, the AFA II individuals were rinsed in a descending ethanol series (90% 3 x 10 min, 70% 2 x 10 min, 50% 2 x 10 min) finishing with a rinsing in distilled water (2 x 10 min minimum). The rinsed samples were infiltrated overnight in the refrigerator in cryoprotectant (25% sucrose in PBS). The formaldehyde fixated individual was rinsed in distilled water (at least 3x10min) and then infiltrated in cryoprotectant as well.

The samples were embedded in a drop of mounting medium (Neg-50) on an uncoated microscope slide placed on the freezing plate (-60^0C) of the cryostat with a pre-established orientation (mouth pieces toward the side and the ocelli upward). The mounted sample had the bottom end cut so that a straight edge was created. The sample was them removed from the slide and mounted vertically on the straight edge in the same medium on a specimen holder. This in turn was removed from the freezing plate and left inside the cryostat for 15 minutes to slightly warm up in order to reach the optimal sectioning temperature. The sections were manually placed on a kromalungelatine microscope slide. The slide was in turn warmed up so that the sections will melt and thus avoid freeze-drying of the tissue.

Fixation, plastic embedding and sectioning

For the plastic embedding, two Turnip and two Bogong moths were used. The scales mouthpieces, antennae as well as large portions of the eyes were removed in order to improve fixative penetration. The samples were fixated overnight in the refrigerator in a modified Karnovsky solution (2.5% Glutaraldehyde + 2% paraformaldehyde in 0,1 M sodium cacodylate buffer of pH ca 7,4). After the fixation was completed, the samples were rinsed in in 0.1 M sodium cacodylate buffer and dehydrated in an ethanol series (70% etoh 2x10 min, 96% etoh 2x10 min, 100% etoh 2x10 min). The embedding of the samples occurred according to the following series: acetone 2x15 min, aceton/epon 2:1 (2+1) 30 min, aceton/epon 1.2 (1+2) overnight, epon 6h and finished in an embedding in new epon molds. The molds were in turn polymerized in the oven at 60^0C for 48h.

The ocelli were sectioned perpendicular to the height of the ocellus. These three micrometer sections were placed in water drops on a microscope slide coated with kromalungelatine and stretched on a warm plate. These were stained in a Richardssons Metylenblue for ten seconds, rinsed in distilled water and dried on the warm plate. The process was completed with the mounting of a coverslip with New Entellan.

Image analysis

The obtained images from the stereomicroscopy, plastic sectioning and hanging drop methods were performed using the software Fiji version v.1.51a x64.

Lateral and perpendicular images of the ocelli were obtained using the Nikon SMZ18 stereomicroscope. Thus, for the lateral view images, the total height of the ocellus and the thickness of the lens above the cuticula were measured. By doubling the measured thickness of the visible part of the lens, an approximation of the total thickness of the lens was obtained. The perpendicular diameters passing through the center of the lens were measured on the images in which the ocellus was photographed directly from above. These represent the width of the ocellus.

The plastic sections provided measurements of the lens thickness and width, as well as the total length of the ocellus and the distance to the photoreceptor layer. For the Turnip moth, the measurements come from different sections of the same ocellus, whereas for the Turnip moth, the sections came from two different ocelli.

The optical properties of the ocelli

The hanging-drop method used by Warrant et al (2006) was employed to measure the back focal distances (BFD) and focal lengths (*f*) of the ocellar lenses. The ocelli lens together with a small portion of the surrounding capsule were carefully dissected and placed in a petri dish of water. By using an eyelash glued to a toothpick, the lens was cleaned from any tissue and pigment. An o-ring was waxed to a conventional microscope glass and its upper surface was lightly greased with Vaseline. The cleaned ocellus was placed with its external side outwards in a tiny drop of water (refractive index = 1.34) on the center of a microscope cover slip, which in turn was placed upside down onto the greased o-ring. Thus, an air-tight chamber was created. The microscope slide was mounted on the stage of a conventional light microscope (Leica) that had its condenser removed. Dark stripes of known size on translucent tracing paper of were placed on the foot of the microscope, over the lamp aperture. These objects focused by the ocellus were viewed with the 40x objective and photographed with a digital camera fitted to the microscope.

The following equation was used to calculate the focal length *f* of each ocellus:

$$f = s_o \frac{\lambda_i}{\lambda_o}$$

where the s_o is the distance between the striped object and the ocellus (127 mm), λ_o is the spatial wavelength of the striped pattern (the distance between the center of one stripe and the center of the next: 4 mm) and λ_i is the spatial wavelength of the image of the striped pattern (mm). Multiple photographs were taken for each dissected ocellus. Three measurements were performed on each image in which the striped pattern was clearly in focus.

The distance from the back of the ocellar lens to the plane of best focus (the optical back focal distance, BFD) was measured by first focusing upon small particles of debris attached to the back of the lens, followed by focusing upwards until the best image of the striped object was obtained. The difference in micrometers between these two focus points was measured using a micrometer gauge attached to the microscope stage. The mean value was obtained from nine consecutive measurements for each ocellus, which in turn was corrected for the refractive index of water, by multiplication by 1.34.

Descriptive statistics of the obtained data as well as graphical illustrations were performed using IBM SPSS statistics v.22 x64.

Analysis of brain projections from ocelli

Neurobiotin injections

During the experiment, five Turnip and four Bogong moths were prepared. Each individual was restrained by taping the thorax tightly to a plastic holder to prevent any movement. The head and thorax were fixed with wax, and the majority of the scales on the head were manually removed. The tip of each ocellus containing the lens was carefully removed in order to expose the inside tissue. Neurobiotin (Vector Laboratories, Burlingame, UK) crystals were applied to the tip of a borosilicate micropipette, which was inserted into each exposed ocellar tissue.

The brain and ocellar optical nerves were dissected, cleaned of any remaining air sacks and fixed overnight at 4^0C in a fixative containing 4% paraformaldehyde (PFA), 0.25% glutaraldehyde, and 2% saturated picric acid (in 0.1 M phosphate buffer).

The brains were washed 4 × 15 min in 0.1M PBS and then incubated with Cy3-conjugated streptavidin (1:1000; Jackson ImmunoResearch, West Grove, PA, USA; catalog number 016-160-084) for three days at 4 ◦ C. After incubation, brains were rinsed 4 × 15 min in PBS + Triton-X (Tx) and 2 × 20 min in PBS, dehydrated in an ascending ethanol series (50, 70, 90, 95 and 100%; 15 min each), treated with a 1:1 mix of 100% ethanol and methyl salycilate for 15 min, and eventually rinsed for at least 35 min in pure methyl salycitate. The prepared brains were mounted in Permount between two coverslips, using plastic spacers to prevent squeezing of the brains.

Imaging

The whole-mount preparations were imaged using a 564 nm Argon laser on a confocal microscope (LSM 510 Meta, Zeiss, Jena, Germany) using a 25× objective (LD LCI Plan-Apochromat 25×/0.8 Imm Corr DIC; Zeiss). We scanned at a frame size of 1024 × 1024 voxels with optical sections every 0.79 µm. The resulting voxel size was 0.4972 x 0.4972 x 0.7914 μm^3 with a field of view covering 509 × 509 µm.

Image analysis and three-dimensional reconstruction

The image stacks of the adjacent moth brains and the ocellar optical nerves sections were aligned and merged in

Amira 5.3.3 software (FEI Visualization Sciences Group, Mérignac Cedex, France; RRID: nif-0000–00262).

The ocellar nerves and their projection fields, together with several other brain structures were manually reconstructed using the tool Wrap in the Segmentation editor as well as the Amira plugin Skeletonize (Beetz et al., 2015). A complete reconstructed brain model was provided by Stanley Heinze in order to better illustrate the obtained results.

Results

Characterization of external morphology of the ocelli

Scanning electron microscopy and stereomicroscopy

The Bogong and Turnip moths have two ocelli placed laterally on the vertex of the head, close to the dorsal margin of the compound eyes and posterior to the antennae. The SEM and stereomicroscopy parts of this study have shown that these are cone shaped with a lens that is slightly oval. Generally, the size of the Bogong moth ocelli are slightly smaller than those of the Turnip moth (Table 1).

In the SEM images, a partial collapse of the lens is present, which is present only in the images B3 and B4 (Figure 1). These images come from the individuals that were anesthetized for 20 to 30 minutes in the freezer. This treatment, always caused a partial collapse of the lens. This collapse would only partially affect the total height of the ocellus, which was not measured on these images. The diameters of the lens are the same, as they are measured from cuticle rim to cuticle rim as shown in image C1 (Fig. 1) In the SEM images in Figure 1, originating from the same individual, the height of the ocellus and width of the lens are between 9,7% and 40% larger than those obtained from the stereomicroscopy images (height 138.5 ± 3.54 µm; width 66.75 ± 12.97 µm; Figure 1, Table 1).

Characterization of the internal morphology of the ocelli

Paraffin, cryo and plastic sections

Three methods were employed to study the internal morphology of the Bogong and Turnip moths. Both the paraffin embedded and cryo-sectioned material suffered from severe fragmentation making it impossible to obtain any data.

The plastic embedding method was somewhat more successful, although even here a high degree of fragmentation was present. Almost none of the connective tissue and photoreceptor layer were preserved in the samples. The ocelli lenses were partially fragmented as well (Figure 1). However, measurements of their thickness and width were possible. Because of the high degree of fragmentations, all the measurements of these samples represent approximations.

The image D4 is based on a toluidine blue stained ocellus sectioned at a thickness of 0.8 micrometers. This was provided to us by Professor Willi Ribi from the Department of Neurobiology, Research School of Biology, ANU, Canberra, Australia.

The measurements of the lens dimensions are similar to those obtained from our own ocelli. However, one difference has been observed: the total height of the ocellus is slightly smaller than those obtained from our own ocelli.

The measurements of the width (75.75 ± 1.5 µm) of the lens and the height (138.5 ± 15.16 µm) of the ocellus are similar in the plastic sections to those obtained from the stereomicroscopy method. The lens thickness is significantly larger in the stereomicroscopy method (92 µm vs.

Table 1. Size measurements of the ocelli and their lenses. A - D represents the Bogong moths and E - F the Turnip moths. The numbers and letters following, represent the image IDs from Figure 1. The measurements are in micrometers. The measured lens dimensions (thickness, width, diameters, height) are illustrated in Figure 1.

Species	Lens				Ocellus	Distance to photoreceptor layer
Image ID	Thickness	Width	Diameter A	Diameter B	Height	
B1	92				141	
B2	92				136	
B3			59	53		
B4			81	74		
C1			89	98		
C2					152	
D1	75	75			145	
D2	72	75			144	
D3	70	78			149	
D4	70	75			116	5
E1	78				122	
E2			62	66		
F1	89	97			135	
F2	90	85			143	

71.75 ± 2.36 µm; *t* test: $t = -11.43$, $df = 4$, $P < 0.001$; Table 1).

In the case of the Bogong moth, the plastic embedded sample provided a lower thickness for the lens compared to the stereomicroscopy measurements, whereas for the Turnip moth, the opposite is true. Compared with each other, the Bogong moth has a higher ocellus (*t* test: $t = 0.16$, $df = 7$ $P = 0.88$; Table 1), but a thinner (*t* test: $t = -1.54$, $df = 7$, $P=0.168$) and narrower (*t* test: $t = -2.52$, $df = 1$, $P=0.23$) lens, although these differences are not statistically significant.

The optical properties of the ocelli

Out of the nine Bogong ocelli studied, three were removed due to lens distortions or low picture quality (Figure 2 Bogong moth). For the first three ocelli, no back focal distance (BFD) was obtained.

The focal length *f* of the lens in the Bogong moth ocelli was found to range between 166 µm and 248 µm. There are differences in the values of each Bogong moth ocellus, with ocelli C (221 ± 2.987 µm) and I (248 ± 5.99 µm) having been the largest (Figure 3d).

Because of these, the focal length data for all ocelli and pictures is not normally distributed. The variation in the data of each ocellus is smaller and normally distributed (Figure 3c, Table 2). The back focal distance data for all ocelli is not normally distributed and neither is the data for ocelli D and F. The mean values vary between a minimum of 15.3 ± 4.03 µm for ocellus D and a maximum of 21.4 ± 3.96 for ocellus F (Table 2).

The focal length for all the Turnip moth ocelli was measured. However, ocellus C had only one picture that was clear enough to permit any measurements (Figure 2 Turnip moth). The mean *f* of the Turnip moth ocelli (183 µm) is smaller than that of the Bogong moth (198 µm ± 34.166) although not statistically different (Mann–Whitney U = 3262.5, n1 = 69 n2 = 111, P=0.095 two-tailed) (Table 2). Contributing to this, is ocellus A (Figure 3b), which has values varying around 225 µm. Except for this ocellus, the differences

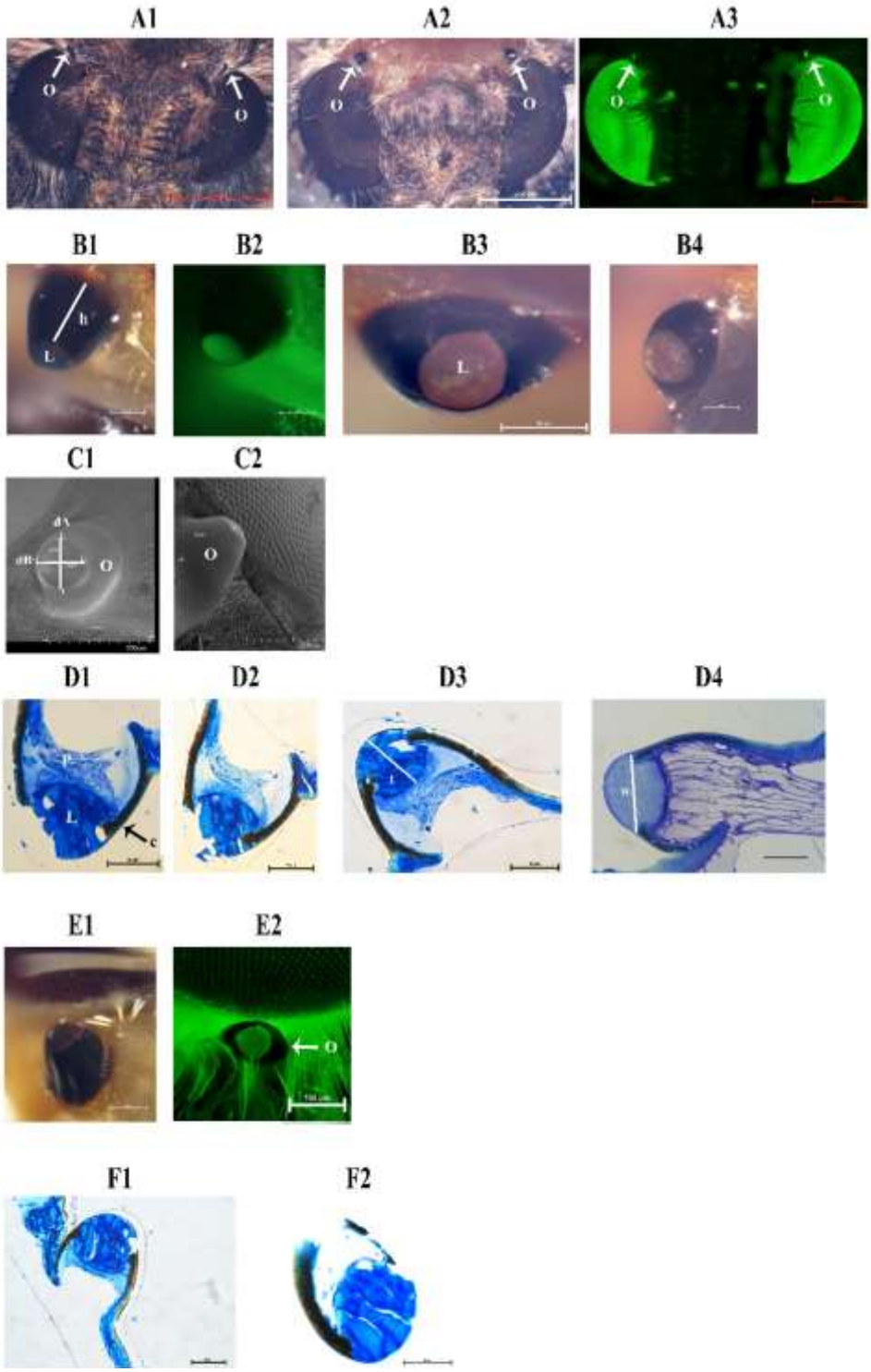

Figure 1. Images on which ocelli size measurements were performed from the stereomicroscopy, SEM and plastic embedding. Panel A: the position of the ocelli on the Bogong moth's head with 1 – scales present, 2 – scales removed, 3 – fluorescent imaging. Panel B: Bogong moth ocelli used in measurements, image 2 – fluorescent imaging. Panel C: Bogong moth ocelli SEM imaging. Panel D: Bogong moth ocelli, plastic embedding images 1-3 are from the same individual. Panel E: Turnip moth ocelli, image 2 fluorescent imaging. Panel F: Turnip moth ocelli, plastic embedding, both images come from the same individual. Notations: O – ocellus, L – Lens, P – the photoreceptor layer of the retina, c – chitin sheath of the ocellus, h – measured height of the ocellus, dA&B – the measured diameters of the ocellar lens seen from above, t – the measured thickness of the lens, w – the measured width of the lens. Image D4 courtesy of Professor Willi Ribi of the Department of Neurobiology, Research School of Biology, ANU, Canberra, Australia.

Table 2. Size measurements of the optical properties of the ocelli (labeled A-I) for both species. *f* represents the focal distance and BFD back focal distance (p= p-value, N = number of measurements for each ocellus – three measurements/image).

Ocelli ID Optical property	A	B	C	D	E	F	G	H	I	Mean value
Bogong *f*	188 ± 3.51 p=0.87 N=15		221 ± 2.99 p=0.97 N=6	168 ± 4.85 p=0.55 N=3		166 ± 3.57 p=0.88 N=12		169 ± 6.061 p=0.16 N=15	248 ± 5.05 p=0.79 N=18	197.7 ± 34.17 p<0.001 N=69
Bogong BFD				15.3 ± 4.03 p=0.013 N=9	16.4 ± 2.83 p=0.23 N=9	21.4 ± 3.96 p=0.011 N=9	16.8 ± 1.91 p=0.25 N=9	19.1 ± 3.59 p=0,23 N=9	18 ± 3.08 p=0.21 N=9	17.8 ± 3.74 p=0.002 N=54
Turnip *f*	220 ± 6 p=0.51 N=15	164 ± 2.09 p=0.83 N=18	176 ± 4.01 p=0.76 N=3	182 ± 7.78 p=0.09 N=24	179 ± 4.53 p=0.76 N=15	179 ± 4.66 p=0.08 N=15	181 ± 2.6 p=0.48 N=21			183 ± 16.77 p<0.001 N=111
Turnip BFD	18.5 ± 3.95 p=0.24 N=9	20.6 ± 3.61 p=0.74 N=9	20.1 ± 2.84 p=0.39 N=9	23.2 ± 2.84 p=0.30 N=9	22 ± 2.13 p=0.81 N=9	21.6 ± 3.7 p=0.18 N=9	23.2 ± 2.12 p=0.91 N=9			21.3 ± 3.37 p=0.044 N=63

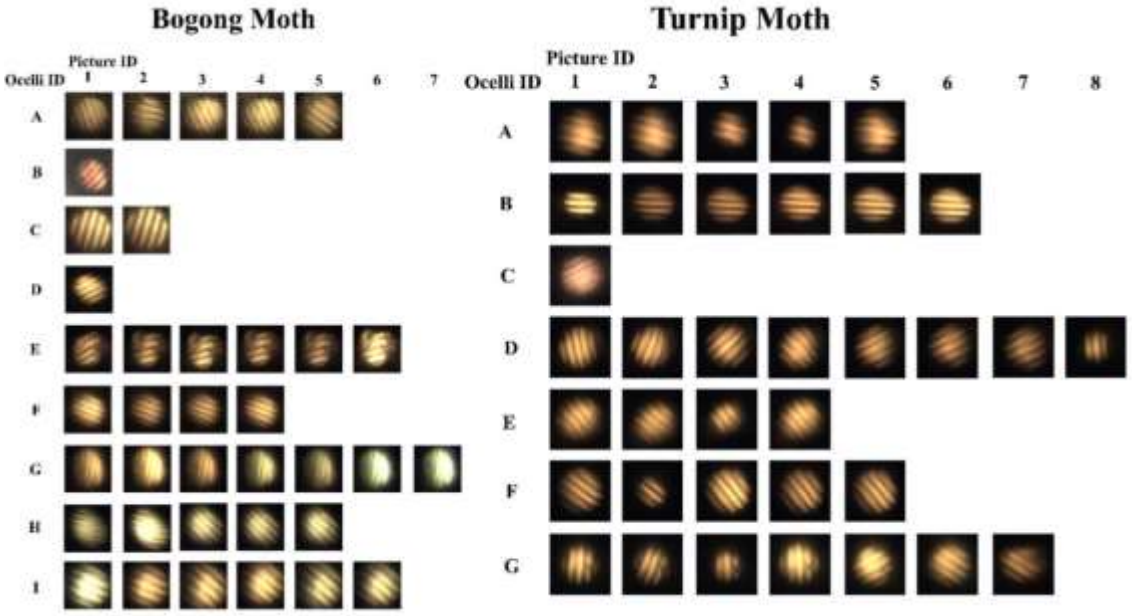

Figure 2. Images on which optical measurements of the ocelli were performed for the Bogong and Turnip moth.

between the values of the remaining ocelli are smaller (Figure 3a).

There is a large overlap between the focal lengths of both species. In Figure 3e the values for ocellus A represent the top outliers for the Turnip moth and the bottom outlier is a value from ocellus D.

The back focal distance values show no normal distribution whereas the values for each individual ocellus are normally distributed (Table 2). The mean values for the back focal distance vary between a minimum of 18.5 ± 3.95 µm for ocellus A and a maximum of 23.2 ± 2.84 µm for ocellus D and 23.2 ± 2.12 µm for ocellus G (Table 2). The back focal distance of the

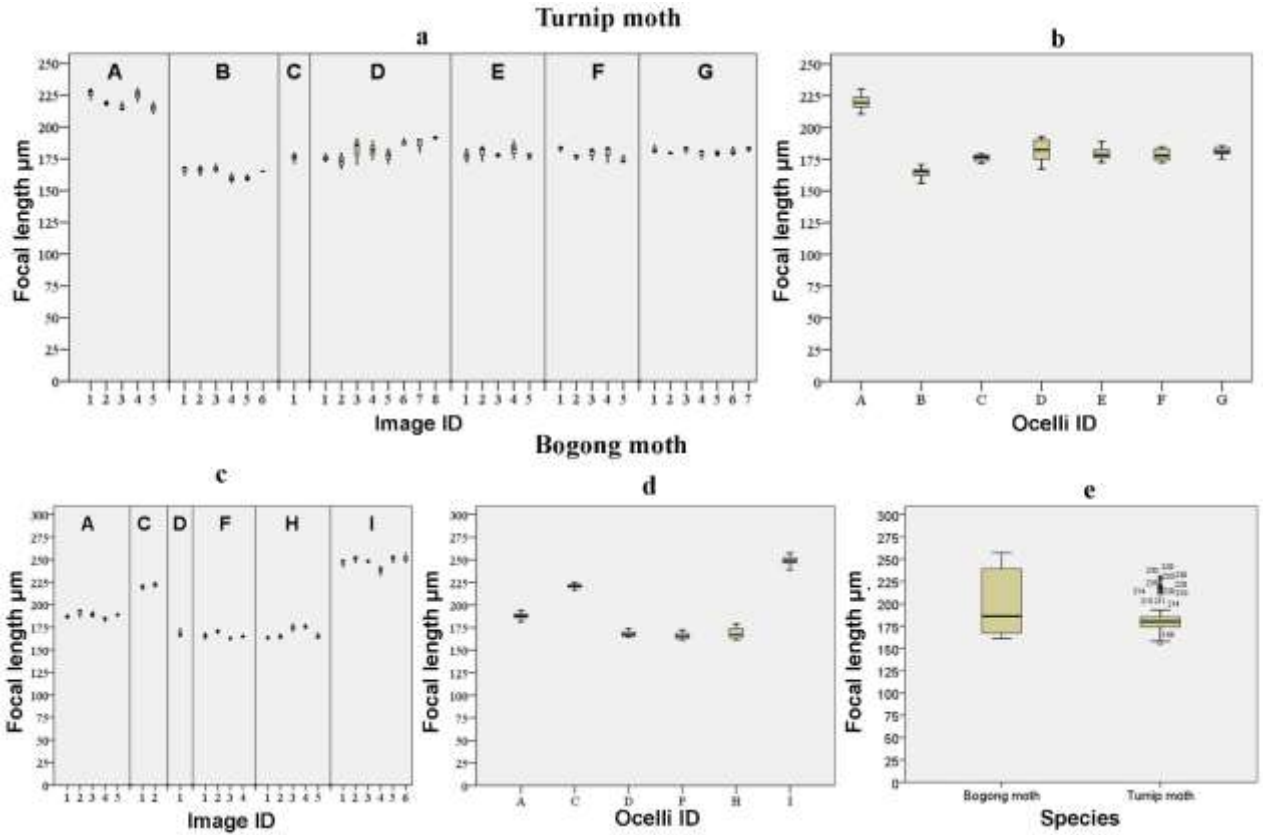

Figure 3. Boxplot graphs illustrating the focal distance data. A, C show all the measurements for each image used for the Turnip and Bogong moth. B, D show all the measurements for each ocellus. E shows all the image data per species. Each outlier represents the measurement size in micrometers.

turnip moth is significantly larger than that of the bogong moth (Mann–Whitney U = 752.5, n1 = 54 n2 = 63, $p<0.001$ two-tailed).

Analysis of brain projections from ocelli

The Neurobiotin injections led to the imaging and reconstruction of both long and short fibers of the Bogong moth ocelli. Thus, from the four prepared brains, two have shown enough detail to enable the reconstruction of both the ocellar neuron bundles as well as important brain parts.

In the first individual, both mushroom body calyxes as well as each pedunculus were reconstructed (Figure 4 A2). The short fibers coming from the ocelli photoreceptor layers follow closely the posterior contours of the mushroom bodies. Approximately one third of the width of the mushroom body calyx the short fibers end, and long neuronal fibers start, four on the right side and three on the left side. The long fibers from the right side divide in half and form one projection field on each side. Out of the three fibers coming from the left side, only one of them forms a projection field on the opposite side. Thus, each projection field contains fibers coming from both sides. In this individual, it was impossible to differentiate between the upper and lower divisions of the central complex. Instead, the overall approximate location of these structures are represented together with the reconstruction of the nodules.

In the analysis of the second individual, it was possible to reconstruct only one of the mushroom body calyxes together with its pedunculus. However, here it was possible to reconstruct the two divisions of the central complex. The path of the short fibers is dorsal the pedunculus and posterior the mushroom body, similar to

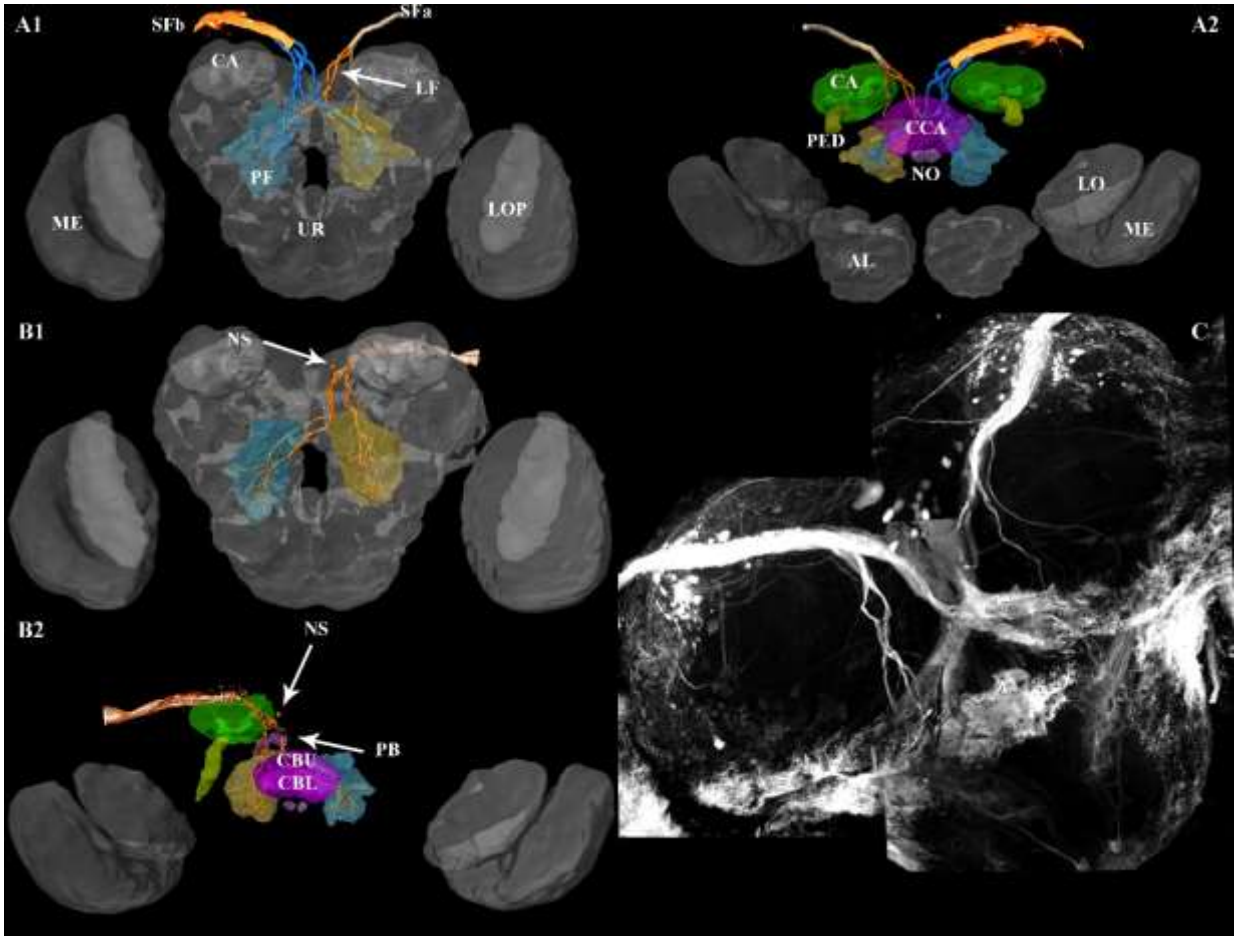

Figure 4. Anterior (A1, B1) and posterior (A2, B2) views of several brain structures and stained Bogong moth ocellar L-neurons. The grey neuropils come from the model brain of this species (used with the permission of Stanley Heinze). The colored neuropils represent my own reconstructions of different brain structures (AL – antennal lobe; CA – calyx body; CCA – central complex area; CBU – central body upper division; CBL – central body lower division; LOP – lobula plate; LO – lobula; ME – medulla; NO – nodules; PB – protocerebral bridge; UR – undefined regions) as well as the short (SFa – neuropil reconstruction SFb – voltex reconstruction) and long fibers (LF) of the ocellar neurons together with a neuron soma (NS).

the path in the first individual (Figure 4 B1&2). In this reconstruction, four long fibers are present that form two projection fields on both the right and left side. These projection fields are anterior of the central complex, posterior to the brain surface and close to the esophageal hole. For this individual it was possible to even reconstruct the soma of a neuron (Figure 4 B1&2 NS).

The long fibers form rather large projection fields in both individuals that are located in the currently undefined regions of the brain. It is very probable that each projection field is formed of at least four long fibers, half of each originating from the right ocellus and half from the left ocellus.

No reconstruction was possible for the Turnip moth due to either damage occurring during the dissection and fixation steps or due to low staining of the nerve cells themselves.

Discussion

The purpose of the present study was to investigate the external and internal morphology of the ocelli in Turnip and Bogong moths as well as the neural projections from these structures. This,

together with comparing these two species with each other, may shed light on the function of these sensory organs.

Characterization of the external morphology of the ocelli

The external morphology of the ocellus is nearly identical in both of the studied species, where the Bogong moth has a slightly higher ocellus. Both species had abnormally large individuals (Bogong moth – A, Turnip moth – I, Figure 3a&c), which affected the mean value of the measurements and skewed the dataset.

Unlike honeybees (Ribi et al., 2011), wasps (Warrant et al., 2006) and dragonflies (Berry et al., 2007), the studied species have only two ocelli, placed laterally on the vertex of the head, close to the dorsal margin of the compound eyes and posterior to the antennae. This location is typical for moths species, but not unique among flying insects (Mizunami, 1994).

In the studied species, the ocellar surface was completely smooth, unlike in honeybees, where between half and two thirds of each lens has a rough surface (Ribi et al., 2011). In the present study, any lens surfaces that were not smooth were caused by partial collapses of the surface, due to the treatment of the sample.

This was observed in all the SEM prepared samples. The same effect can be seen in the images obtained by Grunewald and Wunderer in 1996. The measurements performed using this method are not entirely accurate due to distortions, not due to individual size variation. It can be seen that the diameters of the lens were with approximately 20 micrometers larger in the SEM sample compared with the stereomicroscopy samples (Table 1). If the ocellar lenses of the honeybees (Hung and Ibbotson, 2014), orchid bees (*Euglossa imperialis*) (Taylor et al., 2016) and lateral dragonflies (lateral ocellus: Berry et al., 2007)ocelli are asymmetrical, the lenses of Turnip moths and Bogong moths are rather symmetrical.

Characterization of the internal morphology of the ocelli

Unlike the external surface of the lens, the internal ocellar surface of the Bogong moth (as seen in the plastic embedded sections) is less symmetrical and rather flat with no pronounced curvature like that found in the honeybee ocelli (Hung and Ibbotson, 2014), as seen in the plastic embedded sections. This can be observed from our measurements as well, where the thickness is generally smaller than the diameter (Table 2).

The fact that the ocellar lens is not perfectly spherical results from the differences between the two perpendicular diameters of the lens. This however, cannot be seen in the plastic sections, as these were performed in the longitudinal plane of the ocellus.

Because of the shape of the lens, the retinal is also different from that of the honeybees (Ribi et al., 2011), which presents a division into a dorsal and a ventral surface. The vitreous body underlying the retina forms a thin and uniform layer, that closely follows the shape of the lens. Because of the high degree of fragmentation in our plastic sections, no more information can be obtained about the internal structure of the Bogong moth ocelli. Information about the internal structure of the Turnip moth ocelli, is missing as well, although there is a high probability that is very similar to that of the Bogong moth, due to the overall similar external shape and dimensions.

What caused this high degree of fragmentation and poor fixative penetration in our preparations is still unknown. The fact that these samples had large parts of their eyes removed as well, did not seem to improve the results. The same large degree of fragmentation was present as in the paraffin and cryo sections.

The method used is common for insect plastic embedding. Another possible explanation may be the thickness of the slice, as our slices were three micrometers thick versus 0.8 micrometers (as used for D4 sample.

The dimensions of the lens are similar between the D4 individuals and those obtained by me. The height of the D4 ocellus was smaller than those the studied ocelli. However, this may be explained by individual size variation or distortions in my sections.

Why the cryo sectioning and paraffin embedding methods did not work, is still unknown, although poor fixative penetration seems likely to be the probable cause.

The optical properties of the ocelli

The optical properties of the ocelli were investigated by measuring the focal length *f* and back focal distance BFD of the lens. The measurements obtained from both species are rather similar. Thus, the Bogong moths which have a thinner and narrower lens, had a larger focal length (197.7 µm), whereas the back focal distance was smaller (17.8 µm) than the Turnip moth (*f* = 183 µm and BFD = 21.3 µm, Table 2).

In our study, we found no astigmatism like that present in honeybees (Ribi et al., 2011), the nocturnal sweat bee (*Megalopta genalis*), the nocturnal paper wasp (*Apoica pallens*) or the diurnal paper wasp (*Polistes occidentalis*) (Warrant et al., 2006). Thus, the ocelli of our species havethe same focal plane for each axis of the lens, which in the case of the Bogong moth, lies well behind the retina whose distal surface lies 5 microns behind the rear surface of the lens. Due to unsuccessful plastic sectioning, it is still unknown if the Turnip moth ocelli are also underfocused, although it is probable, due to the even higher back focal distance. Our findings are similar to those for other insect species such as locusts, flies and dragonflies, which possess underfocused ocelli as well (Stange et al., 2002). There are however some exceptions such as the orchid bees (*Euglossa imperialis*) (Taylor et al., 2016) as well as the nocturnal sweat bee (*Megalopta genalis*), the nocturnal paper wasp (*Apoica pallens*) or the diurnal paper wasp (*Polistes Occidentalis*) (Warrant et al., 2006) in which the focal plane of the lens is projected on the retina.

Neural ocellar projections

The number of neurons projecting from each ocellus in our preparations, was found to be between three and four. Typically, half of these form projections fields on the ipsilateral side of the brain (close to the esophageal), whereas the other half project to the contralateral side of the esophageal hole. The diameters of these fibers are very large and their numbers low. Comparison with other species is difficult, as most studies have been done on tri-ocellar species with divided retinas (created by due to a strong curvature of the inner surface of the ocellar lens).

It is worth mentioning that both the descending ocellar neurons of both dragonflies and honeybees also form projection fields in the area around the esophageal hole. However, unlike our findings, the neurons of these species often descend lower into the suboesophageal ganglion (Berry et al., 2006;Berry et al., 2007;Hung and Ibbotson, 2014). In our species, the projection fields of the descending large second order neurons (L_D-neurons) are found in the currently undefined regions of the brain, where no known brain structures have as yet been defined.

The role of the ocelli in Bogong and Turnip moths

The ocelli of the Bogong moths are strongly underfocused and there is a high probability that this is also true for the Turnip moths as well. Because of this, it is

highly improbable that the poor spatial resolution enables these two species to use their ocelli for navigation using patterns such as the spatial pattern of leaves in a forest canopy.

Without a more detailed study of the rhabdoms of these two species, it is impossible to say with any degree of certainty whether the ocelli are capable of detecting any pattern of skylight polarization. However, the brain projection fields found in the present study, make celestial polarization analysis improbable as well. In other insects, polarization sensitive ocelli have L_D-neurons that project into either the optic lobe, the anterior optic tubercle or the central complex (el Jundi et al., 2014). Our neurons project to neither of these polarized light processing structures.

The size and number of the L_D-neurons, reveal that they have a high information convergence as well as very fast signal propagation. These characteristics, may point to a role of the ocelli in flight stabilization reflexes, by directly connecting the ocelli to the motor centers of the brain. This of course may prove beneficial for both a migratory as well as a non-migratory species.

The two laterally positioned ocelli of Cabbage and Arctiid moths (Grunewald and Wunderer, 1996; Pappas and Eaton, 1977) have been shown to perform an important function in the circadian regulation of diurnal activities (Eaton et al., 1983; Sprint and Eaton, 1987; Yamazaki and Yamashita, 1991). Typical for the ocelli of many species, the ocellar lens of the Arctiid moths creates an image plane that lies behind the retinal layer (Grunewald and Wunderer, 1996; Mizunami, 1994).

These findings are similar to those in the two species studied here. Thus, another role for the ocelli may be to regulate the initiation and cessation of diurnal activities such as flight, as found in the Cabbage looper moth and in Arctiid moths (Eaton et al., 1983;Sprint and Eaton, 1987). A highly light sensitive organ that can accurately control the initiation and cessation of diurnal activities, is most certainly advantageous to a long distance migratory species such as the Bogong moth, for which the timing of nocturnal migratory flight is important.

There are still many questions to be answered, before a definite role for the ocelli can be assigned in these two species. This can only be achieved by further research on the structure of the retina and photoreceptors, the size and extent of the visual fields of the lenses, and the responses of ocellar neurons to different light stimuli.

Acknowledgements

I thank my supervisors Eric Warrant and Stanley Heinze for offering me the opportunity to conduct this study, for providing the necessary equipment and for their invaluable guidance. I also thank Carina Rasmussen and Ola Gustafsson for their help with the laboratory methods, plastic embedding and sectioning and the SEM preparation and analysis of the samples. I also thank Willi Ribi for allowing me to use one of his images of the plastic sections of the ocellus of the Bogong moth.

References

Beetz, M. J., el Jundi, B., Heinze, S. and Homberg, U. (2015). Topographic organization and possible function of the posterior optic tubercles in the brain of the desert locust Schistocerca gregaria. *J. Comp. Neurol.* **523,** 1589-1607.

Berry, R. P., Stange, G. and Warrant, E. J. (2007a). Form vision in the insect dorsal ocelli: An anatomical and optical analysis of the dragonfly median ocellus. *Vision Res.* 47, 1394-1409.

Berry, R. P., Warrant, E. J. and Stange, G. (2007b). Form vision in the insect dorsal ocelli: An anatomical and optical analysis of the Locust Ocelli. *Vision Res.* 47, 1382-1393.
Berry, R. P., Wcislo, W. T. and Warrant, E. J. (2011). Ocellar adaptations for dim light vision in a nocturnal bee. *J. Exp. Biol.* 214, 1283-1293.
Berry, R., Stange, G., Olberg, R. and van Kleef, J. (2006). The mapping of visual space by identified large second-order neurons in the dragonfly median ocellus. *J. Comp. Physiol. A -Neuroethol. Sens. Neural Behav. Physiol.* **192,** 1105-1123.
Berry, R., van Kleef, J. and Stange, G. (2007). The mapping of visual space by dragonfly lateral ocelli. *J. Comp. Physiol. A -Neuroethol. Sens. Neural Behav. Physiol.* 193, 495-513.
Britton, D. Agrotis infusa Bogong Moth (Boisduval, 1832) . *Atlas Of Living Australia* 2016,.
Caldwell, J. C., Fineberg, S. K. and Eberl, D. F. (2007). Reduced ocelli encodes the leucine rich repeat protein Pray For Elves in Drosophila melanogaster. *Fly* 1, 146-152.
Chen, Q. and Hua, B. (2014). Ultrastructure of dorsal ocelli of the short-faced scorpionfly Panorpodes kuandianensis (Mecoptera: Panorpodidae). *Micron* 59, 8-16.
Chumakov, M. A. and Kuznetsova, T. L. (2008). Pests Agrotis segetum (Denis & Schiffermueller) - Turnip Moth. *Interactive Agricultural Ecological Atlas of Russia and Neighboring Countries. Economic Plants and their Diseases, Pests and Weeds* 2016,.
CSIRO. Bogong Moth Agrotis infusa. *Melbourne Museum* 2016,.
Dickens, J. C. and Eaton, J. L. (1974). Fine-Structure of Ocelli in Sphinx Moths. *Tissue Cell* 6, 463-470.
Dickens, J. and Eaton, J. (1973). External Ocelli in Lepidoptera Previously Considered to be Anocellate. *Nature* 242, 205-206.
Dow, M. and Eaton, J. (1976). Fine-Structure of Ocellus of Cabbage-Looper Moth (Trichoplusia-Ni). *Cell Tissue Res.* 171, 523-533.
Eaton, J. (1971). Insect Photoreceptor - Internal Ocellus is Present in Sphinx Moths. *Science* 173, 822-&.
Eaton, J. (1976). Spectral Sensitivity of Ocelli of Adult Cabbage-Looper Moth, Trichoplusia-Ni. *Journal of Comparative Physiology* 109, 17-24.
Eaton, J., Tignor, K. and Holtzman, G. (1983). Role of Moth Ocelli in Timing Flight Initiation at Dusk. *Physiol. Entomol.* 8, 371-375.
el Jundi, B., Pfeiffer, K., Heinze, S. and Homberg, U. (2014). Integration of polarization and chromatic cues in the insect sky compass. *J. Comp. Physiol. A -Neuroethol. Sens. Neural Behav. Physiol.* **200,** 575-589.
Fent, K. and Wehner, R. (1985). Ocelli - a Celestial Compass in the Desert Ant Cataglyphis. *Science* 228, 192-194.
Grunewald, B. and Wunderer, H. (1996). The ocelli of arctiid moths: Ultrastructure of the retina during light and dark adaptation. *Tissue Cell* 28, 267-277.
Horie, T., Sakurai, D., Ohtsuki, H., Terakita, A., Shichida, Y., Usukura, J., Kusakabe, T. and Tsuda, M. (2008). Pigmented and nonpigmented ocelli in the brain vesicle of the ascidian larva. *J. Comp. Neurol.* 509, 88-102.
Hu, K. and Stark, W. (1980). Roles of Drosophila Ocelli and Compound Eyes in Phototaxis. *Journal of Comparative Physiology* 135, 85-95.
Hung, Y. and Ibbotson, M. R. (2014). Ocellar structure and neural innervation in the honeybee. *Front. Neuroanat.* **8,** 6.
Kalmus, H. (1946). Correlations between flight and vision, and particularly between wings and ocelli, in insects. *Proceedings of the Royal Entomological Society of London (A)* 20, .84-96.
Lindauer, M. and Schricker, B. (1963). On the function of ocelli in twilight flight of the honey bee. *Biol. Zentralbl.* 82, 721-725.

Mizunami, M. (1994). Information-Processing in the Insect Ocellar System - Comparative Approaches to the Evolution of Visual Processing and Neural Circuits. *Advances in Insect Physiology, Vol 25* 25, 151-265.
Mizunami, M. (1995). Functional Diversity of Neural Organization in Insect Ocellar Systems. *Vision Res.* 35, 443-452.
Pappas, L. G. and Eaton, J. L. (1977). The internal ocellus of Manduca sexta: electroretinogram and spectral sensitivity. *J. Insect Physiol.* 23, 1355-1358.
Pappas, L. and Eaton, J. (1977). Large Ocellar Interneurons in Brain of Cabbage-Looper Moth Trichoplusia-Ni (Lepidoptera). *Zoomorphologie* 87, 237-246.
Rence, B., Lisy, M., Garves, B. and Quinlan, B. (1988). The Role of Ocelli in Circadian Singing Rhythms of Crickets. *Physiol. Entomol.* 13, 201-212.
Ribi, W., Warrant, E. and Zeil, J. (2011). The organization of honeybee ocelli: Regional specializations and rhabdom arrangements. *Arthropod Struct. Dev.* **40,** 509-520.
Schmitt, F., Stieb, S. M., Wehner, R. and Roessler, W. (2016). Experience-related reorganization of giant synapses in the lateral complex: Potential role in plasticity of the sky-compass pathway in the desert ant Cataglyphis fortis. *Dev. Neurobiol.* 76, 390-404.
Schricker, B. U. R. K. H. A. R. D. (1965). The orientation of the honey bee at dawn. And at the same time a contribution to the question of ocelli function in bees [Engl. summ.]. *Z Verglei Chende Physiol* 49, 420-458.
Schwarz, S., Albert, L., Wystrach, A. and Cheng, K. (2011a). Ocelli contribute to the encoding of celestial compass information in the Australian desert ant Melophorus bagoti. *J. Exp. Biol.* **214,** 901-906.
Schwarz, S., Wystrach, A. and Cheng, K. (2011b). A new navigational mechanism mediated by ant ocelli. *Biol. Lett.* **7,** 856-858.
Sprint, M. and Eaton, J. (1987). Flight Behavior of Normal and Anocellate Cabbage Loopers (Lepidoptera, Noctuidae). *Ann. Entomol. Soc. Am.* 80, 468-471.
Stange, G. (1981). The Ocellar Component of Flight Equilibrium Control in Dragonflies. *Journal of Comparative Physiology* 141, 335-347.
Stange, G., Stowe, S., Chahl, J. and Massaro, A. (2002). Anisotropic imaging in the dragonfly median ocellus: a matched filter for horizon detection. *J. Comp. Physiol. A -Neuroethol. Sens. Neural Behav. Physiol.* 188, 455-467.
Taylor, G. J., Ribi, W., Bech, M., Bodey, A. J., Rau, C., Steuwer, A., Warrant, E. J. and Baird, E. (2016). The Dual Function of Orchid Bee Ocelli as Revealed by X-Ray Microtomography. *Curr. Biol.* **26,** 1319-1324.
The Cooperative Research Centre for National Plant Biosecurity. Turnip moth (*Agrotis segetum*) Threat Data. *CRCPlantbiosecurity*.
Toh, Y. and Okamura, J. (2007). Morphological and optical properties of the corneal lens and retinal structure in the posterior large sternma of the tiger beetle larva. *Vision Res.* 47, 1756-1768.
van Kleef, J., James, A. and Stange, G. (2005). A spatiotemporal white noise analysis of photoreceptor responses to UV and green light in the dragonfly median ocellus. *J. Gen. Physiol.* 126, 481-497.
Vrsansky, P. (2008). Central ocellus of extinct cockroaches (Blattida: Caloblattinidae). *Zootaxa*, 41-50.
Warrant, E. J., Kelber, A., Wallen, R. and Wcislo, W. T. (2006). Ocellar optics in nocturnal and diurnal bees and wasps. *Arthropod Struct. Dev.* 35, 293-305.
Warrant, E., Frost, B., Green, K., Mouritsen, H., Dreyer, D., Adden, A., Brauburger, K. and Heinze, S. (2016). The Australian Bogong Moth Agrotis infusa: A Long-Distance Nocturnal Navigator. *Front. Behav. Neurosci.* 10, 77.
Wehner, R. and Strasser, S. (1985). The Pol Area of the Honey Bees Eye -

Behavioral Evidence. *Physiol. Entomol.* 10, 337-349.
Wehrhahn, C. (1984). Ocellar Vision and Orientation in Flies. *Proceedings of the Royal Society Series B-Biological Sciences* 222, 409-411.
Wellingt.WG. (1974). Bumblebee Ocelli and Navigation at Dusk. *Science* 183, 550-551.
Wilson, M. (1978). Functional Organization of Locust Ocelli. *Journal of Comparative Physiology* 124, 297-316.
Wunderer, H. and Dekramer, J. (1989). Dorsal Ocelli and Light-Induced Diurnal Activity Patterns in the Arctiid Moth Creatonotos-Transiens. *J. Insect Physiol.* 35, 87-95.
Yamazaki, S. and Yamashita, S. (1991). Efferent Control in the Ocellus of a Noctuid Moth. *J. Comp. Physiol. A-Sens. Neural Behav. Physiol.* 169, 647-652.